Design optimization of FGM beam in stability problem

Igor V. Andrianov
Institute of General Mechanics, Rheinisch Westfalische Technische Hochschule Aachen, Aachen, Germany

Jan Awrejcewicz
Department of Automation, Biomechanics and Mechatronics, Lodz University of Technology, Lodz, Poland, and

Alexander A. Diskovsky
Department of Higher Mathematics, National Metallurgical Academy of Ukraine, Dnepropetrovsk, Ukraine

Received 2 March 2018
Revised 10 July 2018
17 August 2018
23 September 2018
Accepted 24 September 2018

Abstract

Purpose – The purpose of this paper is to define and solve the problem of an optimized structural topology of the simply supported beam made from functionally graded material (FGM) enabling achievement of a maximum buckling load.

Design/methodology/approach – Two kinds of inclusions are considered: regular distribution of inclusions of different rigidities and non-uniform distribution of identical inclusions. It is shown that the optimal conditions are similar for both structural designs. The optimization problems are solved by using the homogenization method, and the target functions belong to the class of piece-wise continuous functions. Both optimized structures exhibit border zones free of any inclusions, and the largest amount of inclusions is localized in the central zone of the beams.

Findings – It has been shown that the final result of the carried out optimization of the internal structure for both studied types of FGM are similar. The relative increase in the buckling force of the FG beam with the optimized internal structure is on amount of 20 per cent while comparing it with the regular structure beam.

Originality/value – In contrary to a standard approach, this paper is aimed to detect and study a scenario of transition from heterogeneous to its counterpart homogeneous beam structure based on the consideration of the FGM inclusions. In addition, the problem of inversed transition from the optimized homogeneous structure to the optimal heterogeneous one is solved.

Keywords Homogenization, Optimization, Inclusion, Stability, Functionally graded material, Functionally graded beam

Paper type Research paper

1. Introduction

Functionally graded materials (FGMs) can be defined as advanced composite materials fabricated in a way to have graded variation of the relative volume or concentration fractions of the constituent materials (Suresh and Mortensen, 1998). FGMs can be promising in several applications, especially in aviation and rockets industries, where beams are widely used as construction elements. One of the main requirements taken into account in the design of elastic rods is their stability. In the paper, the stability of FGM beams is considered in a bifurcation formulation, which is reduced to the eigenvalue problem of linear ODEs with piecewise constant coefficients. These problems can be solved, for instance, by a transfer matrix method. In the latter case, the resulting transcendental equation is solved

Engineering Computations
© Emerald Publishing Limited
0264-4401
DOI 10.1108/EC-03-2018-0108

numerically. In the case of a single computation, this approach does not present any difficulties, but having in mind an optimal design it is necessary to carry out analysis of a large series of such solutions, which leads to a significant expenditure of computer time. Therefore, an approximate analytical algorithm is preferred to solve the problem.

The recent state-of-the-art regarding the characterization, modeling and analysis of FGM has been reviewed in reference (Victor and Larry, 2007), whereas various aspects of the theory and applications of FGM have been illustrated and discussed in Ramu and Mohanty (2014). The buckling problems of the FGM beams/columns have been overviewed also in monographs (Alfutov, 2000; Elishakoff, 2005; Wang *et al.*, 2005). On the other hand, the buckling problems of FGM columns are reconsidered more recently (Singh and Li, 2009; Huang and Li, 2010; Shahba and Rajasekaran, 2012; Yilmaz *et al.*, 2013).

In the majority of the known works devoted to optimization of the FGM elements, the internal FG structure of the used materials is modeled as a certain homogenous matter with variable parameters along one or two coordinates governed by continuous functions (Banichuk, 1990). Observe that a transition from the input heterogeneous internal structure to its counterpart homogenous one is neither modeled nor described so far. *The present study is aimed at detecting and studying a scenario of the latter transition taking into account the FGM inclusions. In addition, a model of an inverse transition from the being defined optimized homogenous structure to the optimal heterogeneous one, which possesses an important practical advantage, is proposed.*

An approach allowing for getting the macro-scale laws and a constitutive relation by a roper homogenization over the micro-scale is known as a homogenization method (Bensoussan *et al.*, 1978; Babushka, 1979; Sanchez-Palencia, 1980; Bakhvalov and Panasenko, 1989; Manevitch *et al.*, 2002; Movchan *et al.*, 2002; Andrianov *et al.*, 2004; Kolpakov, 2004; Panasenko, 2005). This method is also successfully used for modeling and simulating the mechanical behavior of the FG materials (Reiter *et al.*, 1997; Anthoine, 2010) and the FG structures (FGS). Typically, the term FGS is associated with the constructions made/fabricated from FGM. However, in this paper, the term FGS is understood in a broader manner, as the heterogeneous constructions with a controlled heterogeneity parameter are also taken into account (for instance, the reinforced plates and shells with non-uniformly distributed ribs of different stiffness; corrugated constructions consisting of FG corrugations, etc.) (Andrianov *et al.*, 2005, 2006; 2009, 2010; 2011, 2013).

Andrianov *et al.* (2013) have presented an inverse homogenization method for the design of two-phase (solid/void) FGM microstructures. Bi-directional evolutionary structural optimization technique in the form of inverse homogenization has been used for the design of the FGM (Radman *et al.*, 2013). The common approach for the design of multi-functional materials in these studies is to extremize a linear combination of materials functional properties (Mikhlin, 1964; Cadman *et al.*, 2012). Design for cellular structures consisting of multiple patches of material microstructures using a level set-based topological shape optimization method has been proposed in Keller (1960) and Tadjbakhsh and Keller (1962). More recently Li *et al.* (2018a,b) carry out the topological design optimization of new functionally graded cellular composites with auxetics using a level set method.

The technologies used for the FGM fabrication have been rapidly developing, as new materials are produced all the time (Zhou and Li, 2008). Generally, the materials can be divided into three fundamental groups: layered and fiber-type materials and the materials consisting of inclusions made from material being more or less stiff than the matrix material. As an example, we consider a beam with inclusions shown in Figure 1.

In particular, the results obtained in this research can be either used directly or may serve as a source of ideas to study 1D nanostructures (nanotubes and nanorods) (Keller and Niordson, 1966; Xing and Chen, 2014a, 2014b).

The paper is organized in the following way. Section 2 is devoted to introduction of the mathematical models of the FG elasticity modulus with an emphasis on the FG inclusion sizes and FG steps between inclusions. Optimal design of simply supported composed FG beams is discussed in Section 3. Concluding remarks are presented in Section 4. In Appendix, the error introduced by the two-scale asymptotic method is analyzed in detail.

2. Mathematical models of the FG elasticity modulus

The elasticity modulus E of a two-component beam with a regular internal structure composed of inclusions of the same rigidities and separated by a constant step is defined by the following piece-wise continuous function:

$$E = E_m\left(1 + k\sum_{i=1}^{n}[H[x - \varepsilon(0.5 + i) + \varepsilon_1] - H[x - \varepsilon(0.5 + i) - \varepsilon_1]]\right), \tag{1}$$

where: $H(\ldots)$ is the Heaviside function; $x = X/L$; $k = \frac{E_{inc}}{E_m}$; $\varepsilon = \frac{l}{L}$; $\varepsilon_1 = \frac{\Delta}{2L}$; E_m, E_{inc} are the modulus of elasticity of the matrix and of the inclusions material, respectively.

In a general case, the elasticity modulus (1) of the two-component beam takes the following form:

$$E = E_m\left(1 + k\ \Phi\left(\frac{x}{\varepsilon}\right)\right), \tag{2}$$

where $\Phi(x/\varepsilon)$ is a periodic function of the period ε.

It should be noticed that in the majority of practical cases, a number of inclusions is large, and hence, $\varepsilon \ll 1$.

2.1. FG inclusion sizes

In the considered case (Figure 1a), the coefficient k occurring Equation (1), Equation (2) is defined by a function $k = k(x)$, which describes a way of inclusions change and plays a role of a target function in the problem of optimization of the FG structure.

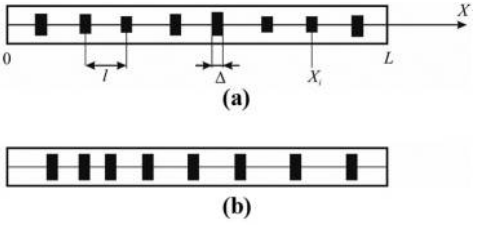

Notes: It is assumed that inclusions are made of one material and with differ in area Ai, $\sum_{i=1}^{n} A_i \equiv const$: (a) FG inclusion sizes: $A_i = A_i(X_i)$, $l_i = l \equiv const$; (b) FG steps between inclusions: $l_i = l(X_i)$, $A_i \equiv const$

Figure 1. A scheme of the two-component beam: l_i - step of inclusions (distance between i-th and (i-1)-th inclusion centers); Δ – inclusion length, $\Delta \equiv const$; X_i is the coordinate of the center of i-th inclusion and $1 \leq i \leq n$, n is the number of inclusions

We begin with a definition of the interval of possible changes of the function $k = k(x)$. It is assumed that the inclusions material is stiffer than the one of the matrix, and hence, $k(x) \geq 0$. Let the value of k_{max} play a role of the upper bound for $k(x)$, where a local buckling may appear between the successive inclusions. Therefore, the bounds of the $k(x)$ function are as follows:

$$0 \leq k(x) \leq k_{max}. \tag{3}$$

To estimate the local buckling load P_l, the internal parts between inclusions can be treated as simply supported beams on their both edges. Furthermore, the classical Euler's load P_L (Andrianov *et al.*, 2006) yields the following estimation of the local buckling load:

$$P_l \sim P_L \varepsilon^{-2}. \tag{4}$$

2.2. FG steps between inclusions

In this case (Figure 1b), the elasticity modulus is presented in the following form:

$$E = E_m \left(1 + k\ \Phi\left(\frac{f(x)}{\varepsilon}\right)\right), \tag{5}$$

where $k = const$. Observe that now $f(x)$ stands for a function defining the change of a step between inclusions.

It is assumed that the number of inclusions is fixed, that is:

$$n = const. \tag{6}$$

Because of reference (Andrianov *et al.*, 2011), the condition in Equation (6) will be satisfied if:

$$f(0) = 0;\ f(1) = 1;\ f'(x) \geq 0, \tag{7}$$

And the step between inclusions can be estimated as follows:

$$l_i \approx 1/f'(x_i).$$

As the condition $f'(x_i) = 0$ implies a lack of the i–th inclusion, the function $f'(x)$ can be interpreted as the target one for inverse problems.

3. Optimal design of simply supported compressed FG beams

A simply supported FG two-component beam (Figure 1) is considered. The beam is compressed by the forces P acting on its ends. Small deformations are assumed and the static Euler method is implemented. To compute the minimum value of the buckling force, the Rayleigh variational principle is used. As a symmetric problem with the same boundary conditions at the beam ends is considered, it is assumed that the possible distribution of the control functions $k(x)$ and $f'(x)$ is symmetric with respect to $x = 0.5$. The symmetry of the problem also implies the symmetry of the buckling form $u(x)$ which yields $u_x(0.5) = 0$.

3.1 FG inclusion sizes

Let us analyze an influence of different size of inclusions on the stability of the FGM beam, keeping the distance between inclusions constant (Figure 1a). The governing self adjoint eigenvalue problem has the following form:

$$u_{xx} + a^{-1} p u = 0, \tag{8}$$

$$u(0) = u(1) = 0, \tag{9}$$

$$\int_0^1 a(x)dx = V; \quad p \to max_k, \tag{10}$$

where: $u(x)$ is the normal beam deflection; $a(x) = \left(1 + k(x)\Phi\left(\frac{x}{\varepsilon}\right)\right)$; $p = \frac{P}{E_m I}$, and I is the moment of inertia of the transversal beam cross-section.

3.1.1 Multi-scale homogenization approach. Usually, the number of inclusions is large; therefore, $\varepsilon \ll 1$ and the problem in Equations (8)-(10) can be simplified with the help of the multi-scale homogenization approach (Bensoussan *et al.*, 1978; Babushka, 1979; Sanchez-Palencia, 1980; Bakhvalov and Panasenko, 1989; Manevitch *et al.*, 2002; Andrianov *et al.*, 2004; Kolpakov, 2004; Panasenko, 2005; Zhang *et al.*, 2006). Let the "fast" variable ξ be introduced in the following way:

$$\xi = x/\varepsilon. \tag{11}$$

The variables x and ξ are treated as independent ones, and the differential operator d/dx has the following form:

$$\frac{d}{dx} = \frac{\partial}{\partial x} + \varepsilon^{-1}\frac{\partial}{\partial \xi}. \tag{12}$$

The eigenfunction u and the eigenvalue p can be presented in the following form:

$$u = u_0(x, \xi) + \varepsilon\, u_1(x, \xi) + \varepsilon^2 u_2(x, \xi) + \ldots; p = p_0 + \varepsilon p_1 + \varepsilon^2 p_2 + \ldots, \tag{13}$$

where the functions $u_s(x, \xi)$, $s = 0, 1, 2, \ldots$ are periodic with respect to ξ and have the non-dimensional period 1; $p_s = const$.

Substituting Equations (11)-(13) into the boundary value problem in Equations (8) and (9), the classical splitting procedure with respect to ε is carried out. As a result, one obtains:

$$\begin{aligned} &u_0 = u_0(x), \qquad u_1 = u_1(x), \\ &u_{2\xi\xi} + u_{0xx} + a^{-1}(x, \xi) p_0 u_0 = 0. \end{aligned} \tag{14}$$

In what follows Equation (14) is integrated with respect to ξ from 0 to 1 while taking into account the periodicity condition for the function $u_2(x, \xi)$. Finally, the problem regarding the maximum buckling force is recast to the following form:

$$u_{0xx} + p_0 \tilde{a}^{-1} u_0 = 0, \tag{15}$$

$$u_0(0) = u_0(1) = 0, \quad u_{0x}(0.5) = 0, \tag{16}$$

$$\int_0^1 \tilde{a}(x)dx = v = const, \quad p_0 \to max_k, \tag{17}$$

Where $\tilde{a}(x) = \left(\int_0^1 a(x)^{-1} d\xi \right)^{-1}$.

The eigenvalue problem in Equations (15) and (17) governs the buckling of the homogenized beam (Figure1a). Besides, the introduced constraint in Equation (3) imply the following inequality:

$$\tilde{a}(x) \geq 1. \tag{18}$$

3.1.2 Stationarity conditions. The stationarity conditions for the boundary value problem in Equations (15)-(18) are derived based on the standard approach reported in reference (Olhoff and Rasmussen, 1977). Namely, multiplying Equation (13) by u_0 and carrying out the integration with an account for the boundary conditions in Equation (14), the following Rayleigh relation is obtained:

$$p_0 = \frac{\int_0^1 u_{0x}^2 dx}{\int_0^1 \tilde{a}^{-1} u_0^2 dx}. \tag{19}$$

Equation (19) implies that the smallest eigenvalue of Equation (15) is equal to the minimum of the functional:

$$p_0 = \int_0^1 u_{0x}^2 dx \tag{20}$$

With the supplementary condition:

$$\int_0^1 \tilde{a}^{-1} u_0^2 dx = 1. \tag{21}$$

The extended Lagrange functional is then introduced by adding the constraints in Equations (17) and (18) to the functional in Equation (20) with the help of the multipliers λ_1, λ_2 in the following way:

$$J = \int_0^1 u_{0x}^2 dx + \lambda_1 \left(\int_0^1 \tilde{a}^{-1} u_0^2 dx - 1 \right) + \lambda_2 \left(\int_0^1 \tilde{a} dx - V \right). \tag{22}$$

Then, the first variation of the functional $\delta J = 0$, generated by variation of the variable $k(x)$, yields the following stationarity condition:

$$u_0^2 = \lambda \tilde{a}^2 \tilde{a}_k^{-1}, \tag{23}$$

where $\lambda = \lambda_2/\lambda_1$.

The stationarity condition in Equation (23) implies the well-posed boundary value problems, which allows for defining the desired functions $k(x)$, $u_0(x)$ and p_0.

The constrains in Equation (18) introduced to the design variable guarantee a satisfaction to the stationarity condition in Equation (23). On the other hand, the symmetry condition regarding the point $x = 0.5$ satisfies Equation (23) for $x_* \leq 0.5$, where $a(x) > 1$, whereas for $0 \leq x \leq x_*$, we have $a(x) = 1$. The latter condition means that there is lack of inclusions in the interval $0 \leq x \leq x_*$. To find the coordinate x_*, the following kinematic conditions (Bakhvalov and Panasenko, 1989) are formulated for the functions $u_0(x)$, $u_{0x}(x)$ at the point $x = x_*$:

$$u_0^- = u_0^+; \quad u_{0x}^- = u_{0x}^+, \tag{24}$$

where $(\cdots)^- = \lim_{x \to x_* - 0} (\cdots); (\cdots)^+ = \lim_{x \to x_* + 0} (\cdots)$.

3.1.3 Example of optimization. Let the function *a(x)* is approximated in the following way:

$$a(x) = \frac{1}{1 - z^2(x) sin^2(\pi n x)}. \tag{25}$$

where $z^2(x) = k(x) < 1$.

In this case, the condition in Equation (17) takes the following form:

$$\int_0^1 \frac{1}{1 - z^2/2} dx = v = const, \tag{26}$$

Equation (15) and the stationarity condition in Equation (23) are governed by the following differential and algebraic equations:

$$u_{0xx} + p_0 (\rho - z^2/2) u_0 = 0, \tag{27}$$

$$z \left(u_0^2 + \frac{2\lambda}{(1 - z^2/2)^2} \right) = 0. \tag{28}$$

However, if the condition of stationarity in Equation (28) is satisfied only because of the second factor, then boundary conditions in Equation (16) will not be satisfied. Therefore, the stationarity condition in Equation (28) with regard to the interval $[0, x_*]$ will be satisfied using only the first factor and assuming $z = 0$ (we take the second factor equal to zero with respect to the interval $[x_*, 0.5]$). The so far mentioned assumptions and simple computations yield:

$$1 - z^2/2 = \begin{cases} 1, & x \in [0, x_*], \\ \dfrac{\sqrt{2\lambda}}{u_0}, & x \in [x_*, 0.5]. \end{cases} \tag{29}$$

Obtaining the function u_0 from the stationarity condition in Equation (29) and substituting it into Equation (27) and conditions in Equation (16) yields the boundary value problem for the control function $z^2(x)$ with regard to the interval $[x_*, 0.5]$:

$$\left(\frac{1}{1-z^2/2}\right)_{xx} + p_0 = 0, \tag{30}$$

$$z(x_*) = 0; \quad z_x(0.5) = 0. \tag{31}$$

Integrating PDE in Equation (30) and taking into account the boundary conditions in Equation (31) yield the following simple algebraic equation:

$$\frac{1}{1-z^2/2} = \frac{p_0}{2}\left(\overline{x}_*^2 - \overline{x}^2\right) + 1, \tag{32}$$

where: $\overline{x} = \frac{1}{2} - x; \quad \overline{x}_* = \frac{1}{2} - x_*$.

Substituting Equation (32) into the isoperimetric condition in Equation (26) allows to define the constant p_0 of the PDE in Equation (30), that is, we have:

$$p_0 = \frac{3(2v-1)}{2\overline{x}_*^3}. \tag{33}$$

To define $\overline{x}_*$, one needs to find u_0 on both intervals $[0, x_*]$ and $[x_*, 0.5]$. For this purpose, we use Equations (27) and Equation (16) for $z = 0$, and taking into account the condition of stationarity in Equation (28), one gets:

$$u_0 = C\sin\sqrt{p_0}x, \quad C = const, \quad x \in [0, x_*]; \tag{34}$$

$$u_0 = \sqrt{2\lambda}\left(\frac{p_0}{2}\left(\overline{x}_*^2 - \overline{x}^2\right) + 1\right), \quad x \in [x_*, 0.5]\ . \tag{35}$$

Substitution of the functions $u_0(x)$ governed by Equations (34) and (35) into the continuity condition in Equation (24) yields:

$$C\sin\left(\sqrt{p_0}x_*\right) = \sqrt{2\lambda}, \tag{36}$$

$$C\cos\left(\sqrt{p_0}x_*\right) = \sqrt{2\lambda p_0}\overline{x}_*. \tag{37}$$

Equations (36) and (37) can be reduced to the following algebraic equation:

$$\sqrt{1 + p_0\overline{x}_*^2}\ \sin\sqrt{p_0}x_* = 1. \tag{38}$$

Finally, substitution of Equation (33) into Equation (38) allows one to get the equation for the size of the border zones being free from inclusions x_*, that is, we have:

$$\sqrt{1+\frac{3}{2}\frac{2v-1}{\bar{x}_*}}\,sin\left(\sqrt{\frac{3}{2}\frac{2v-1}{\bar{x}_*^3}}\frac{1-2\bar{x}_*}{2}\right)=1, \tag{39}$$

where $2v \geq 1$.

It follows from the isoperimetric condition in Equation (26) and solution to Equation (39) that the following inequality should be satisfied:

$$0 \leq \bar{x}_* \leq 0.5. \tag{40}$$

The function $x_* = x_*(v)$ for $v \in [1,10]$ has been found numerically as a solution to Equation (39) satisfying the inequality in Equation (40) and it is shown in Figure 2. As can be seen, the beam boundary layer free from inclusions decreases with increase of v.

In what follows, we quantify the efficiency of the FG beam in comparison to a composite beam of a regular structure. The buckling load or $z=const$ and $\rho - z^2/2 = 1/2v$ has the following simple form:

$$\bar{p}_0 = 2\pi^2 v. \tag{41}$$

A comparison of the buckling load p_0, defined by Equation (33), and the buckling load $\bar{p}_0$ in Equation (41) for $v \in [1,10]$ is reported in Figure 3.

The efficiency of the optimal structure is presented in Figure 3b, where:

$$\delta = \frac{(p_0 - \bar{p}_0)}{\bar{p}_0} \cdot 100\%. \tag{42}$$

The obtained graph clearly shows that efficiency of the employment of the FG beams of the optimal structure, beginning with $v = 1$, practically does not depend on the value of v.

The optimal structure of the FG beam quantified through $a(x)$ governed by Equation (25) is presented in Figure 4 for fixed $\rho = 1$ and $v = 2$.

The inverse transition from the optimal FG homogeneous model in Equations (25) and (29) (Figure 4) to the optimal heterogeneous model (Figure 5) is carried out with the

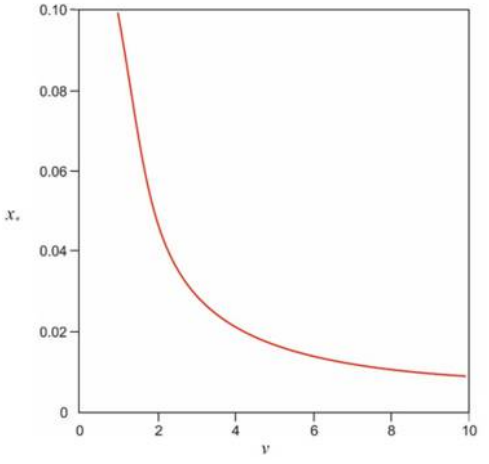

Figure 2.
Coordinate x_* versus v numerically estimated from Equation (39)

help of the following scheme (we consider without loss of generality the case of an even number of inclusions). Namely, the area bounded by the graph of the function $a = a(x)$ (Figure 4) being located above the dotted line $a = 1$ determines the total volume of inclusions:

$$S = 2\int_{x_*}^{0.5} (a(x) - 1)dx. \tag{43}$$

The same area bounded by each wave of the graph is computed in the following way (Figure 4):

$$s_1 = \int_{x_*}^{1/n} (a(x) - 1)dx; \; s_i = \int_{i/n}^{(i+1)/n} (a(x) - 1)dx, \; i = 2, 3, 4, \ldots, n/2. \tag{44}$$

Then there is convenient to introduce the gradient coefficient:

$$r_i = \frac{s_i}{S}, \; i = 1, 2, 3, \ldots, n/2, \tag{45}$$

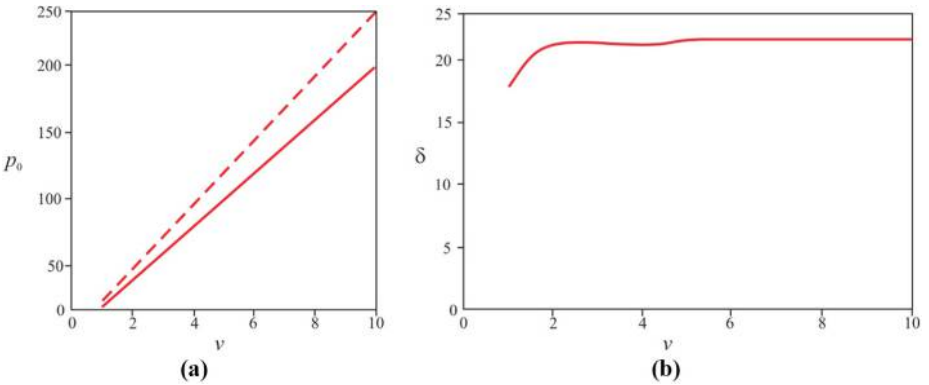

Figure 3.
Buckling loads of the FG beam of the optimal structure Equation (33) and the regular structure composite beam Equation (41) for $v \in [1, 10]$ denoted by dotted and solid lines, respectively, (a) and the function $\delta(v)$ governed by Equation (42) for $v \in [1, 10]$ (b)

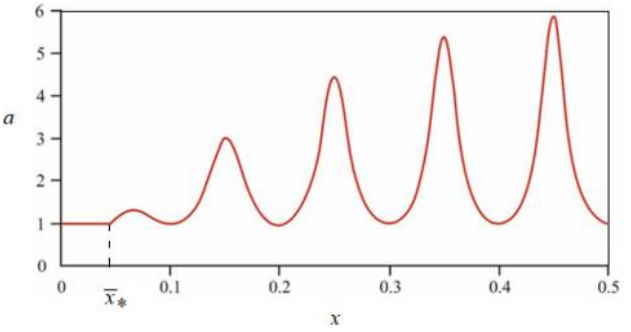

Figure 4.
Optimized structure of FG beam ($\nu = 2$) with parameter in Equation (45)

And the volumes of each inclusion of the FG heterogeneous model are determined via the following simple relation:

$$v_i = r_i V, \tag{46}$$

where V is the given total volume of inclusions of the initial heterogeneous model.

Because of the results presented in Figure 5, one may conclude that the character of the optimized distribution of the inclusions along the beam is close to the character of an optimal distribution of the material of a simply supported beam having a variable transverse cross-section (Fish and Chen, 2001, 2004). The inclusions are concentrated in the middle part of the beam and there is a lack of inclusions in the border zones.

Figure 6 presents the buckling form of the FG optimized beam (solid curve) obtained based on relations in Equations (34) and (35), and the corresponding form for the regular composite beam (dotted curve).

It should be mentioned that the structure with the optimized distribution of inclusions has "a weak zone" in which local buckling may appear before general buckling. It corresponds to the border zone $[0, x_*]$ which does not contain inclusions. The value of the local buckling load p_x can be estimated using the beam of the length x_* with simply supported ends and with the elasticity modulus $\frac{E_m}{\beta}$, that is, in this case, we have:

$$p_{x_*} = \frac{\pi^2}{x_*^{\,2}}. \tag{47}$$

Assuming that the inequality $p_{x_*} \le p_0$ holds, it is clear that the local buckling is possible. Substituting the latter inequality in Equation (47) into Equations (33) and (47), one obtains:

$$x_* \le \frac{3}{2\pi^2}(2v - 1). \tag{48}$$

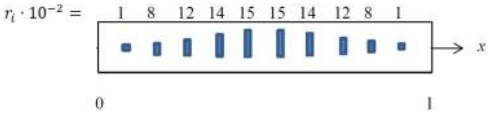

Figure 5. The optimal scheme of the FG two-component beam: r_i ($i = 1, 2, 3, \ldots, 10$) is the gradient coefficient in Equation (45); the volume of the i-th inclusion $v_i = r_i V$, where V is the total volume of inclusions

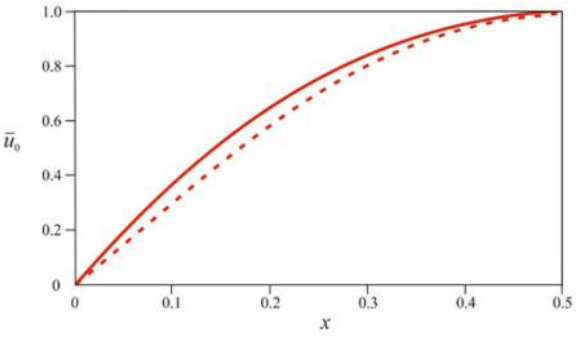

Figure 6. Buckling form $\bar{u}_0$ $(\bar{u}_0 = u_0(x)/u_0(1/2))$ of the FG beam of optimized structure (denoted by a solid curve) and of the regular composite beam (dotted curve)

Substituting the maximum value of x_* governed by Equation (48) into Equation (39) implies that the parameters v, responsible for occurrence of the buckling, should satisfy the following equation:

$$\sin\frac{\pi^3}{3(2v-1)} = -\frac{1}{\sqrt{1+\pi^2}}. \tag{49}$$

The smallest positive root of Equation (49) is as follows:

$$v = 0.732. \tag{50}$$

Because of the reported investigations (Figure 2), x_* monotonously decreases when v increases, which implies the increase in the magnitude of the buckling load of the local buckling. Therefore, Equation (50) indicates that the local buckling is impossible if the following inequality holds:

$$v \geq 0.732. \tag{51}$$

3.2 FG inclusions step

This type of FGM with variable step of inclusions is more suitable in practice than FGM with varying magnitude of inclusions. This is motivated by the fact that from the technological point of view, it is much easier to control the concentration of the same inclusions than to control regularly distributed inclusions with the assumed a priori magnitudes.

Following the earlier considerations given in Section 3.1.4, the following function is derived:

$$a(x) = \frac{1}{\rho - z^2 sin^2\left(\pi n f(x)\right)}, \tag{52}$$

where $z = const$, $z^2 < 1$; $n = const$, which ensures the preservation of the total volume of inclusions.

3.2.1 Multi-scale homogenization approach (concentrated inclusions). The FG beam in which the length of inclusions (Figure 1) is much smaller than the distance between them, that is, the following inequality holds $\Delta \ll min\ l(x)$, is further considered. In such a case, it can be assumed that $\Delta \to 0$, and hence, the inclusions may be treated as concentrated. The stability Equation (8) takes the following form:

$$\left(1 + k\sum_{i=1}^{n}\delta\left(f(x) - i/n\right)\right)u_{xx} + pu = 0, \tag{53}$$

where $k_1 = 2\Delta_1 k$ and δ stands for the Dirac delta function.

Let us introduce the function $\eta = f(x)$. Therefore, $x = f^{-1}(\eta)$, and the stability Equation (53), can be reformulated with respect to η, and it takes the form:

$$\left(1+k_1\sum_{i=1}^{n}\delta(\eta-i/n)\right)\left(\varphi(\eta)^{-1}u_\eta\right)_\eta+\varphi(\eta)pu=0, \tag{54}$$

where $\varphi(\eta)=\frac{d}{d\eta}\left(f^{-1}(\eta)\right)$.

If the function $f(x)$ satisfies conditions in Equation (7), then the boundary conditions in Equation (9) regarding the variable η remain unchanged.

If $\varepsilon=n^{-1}\ll 1$, then the coefficient standing by a higher derivative in Equation (54) serves as a periodic impulse function, and hence, one may apply the multi-scale homogenization approach proposed in reference (Andrianov *et al.*, 2017) (here, the considerations are limited to a smooth step variation between inclusions, that is., we take $f'(x)\sim 1$, and hence, $\varphi(\eta)\sim 1$).

The equilibrium equation of the beam part between the successive inclusions is as follows:

$$\left(\varphi(\eta)^{-1}u_\eta\right)_\eta+\varphi(\eta)pu=0, \tag{55}$$

A conjugate conditions can be written in the following manner:

$$u^+=u^-;\quad u_\eta^+-u_\eta^-=k_1\left(\varphi(\eta)^{-1}u_\eta\right)_\eta, \tag{56}$$

where: $(\dots)^-=\lim_{\eta=i-0}(\dots)$; $(\dots)^+=\lim_{\eta=i+0}(\dots)$.

Because of the multi-scale homogenization approach, the fast variable can be introduced in a classical way:

$$\zeta=\eta/\varepsilon. \tag{57}$$

As the variables η and ζ are treated as independent ones, the differential operator $d/d\eta$ has the following form:

$$\frac{d}{d\eta}=\frac{\partial}{\partial\eta}+\varepsilon^{-1}\frac{\partial}{\partial\zeta}. \tag{58}$$

The eigenfunction u and the eigenvalue p are taken in the following series forms:

$$u=u_0(\eta,\zeta)+\varepsilon u_1(\eta,\zeta)+\varepsilon^2u_2(\eta,\zeta)+\dots;\ p=p_0+\varepsilon p_1+\varepsilon^2p_2+\dots, \tag{59}$$

where $u_s(\eta,\zeta), s=0,1,2,[\dots]$ are periodic with respect to ζ and with period ε.

Substituting Equations (58) and (59) into Equations (55) and (56) and comparing the coefficients standing by the same powers of ε, one obtains:

$$u_0=u_0(\eta),\qquad u_1=u_1(\eta), \tag{60}$$

$$u_{2\zeta\zeta}+\varphi(\eta)\left(\varphi(\eta)^{-1}u_{0\eta}\right)_\eta+\varphi^2(\eta)p_0u_0=0, \tag{61}$$

$$u_2\Big|_{\zeta=1} = u_2\Big|_{\zeta=0}, \tag{62}$$

$$u_{2\zeta}\Big|_{\zeta=1} - u_{2\zeta}\Big|_{\zeta=0} = k\Big(\varphi(\eta)^{-1}u_\eta\Big)_\eta. \tag{63}$$

Observe that in Equation (63), it has been assumed $\overline{k}\sim\varepsilon$. Equation (61), boundary conditions in Equation (9) and conjugate conditions in Equation (62), yields:

$$u_2 = -\Big(\varphi(\eta)\Big(\varphi(\eta)^{-1}u_{0\eta}\Big)_\eta + \varphi^2(\eta)p_0u_0\Big)\zeta(\zeta-1)/2. \tag{64}$$

Substituting Equation (64) into condition in Equation (63), one obtains:

$$\big(\varphi(\eta)+k_1\big)\big(\varphi(\eta)^{-1}u_{0\eta}\big)_\eta + \varphi^2(\eta)p_0u_0 = 0. \tag{65}$$

Coming back to the variable x in the averaged Equation (65), one gets:

$$\Big(1+f^{'}(x)k_1\Big)u_{0xx} + p_0u_0 = 0. \tag{66}$$

3.2.2 Optimal beam design. Let us define the internal structure of the FG beam keeping the maximum buckling load as follows:

$$\int_0^1 y^2dx = \overline{k}, \tag{67}$$

where $y^2 = \overline{k}f^{'}(x)$. The function $y = y(x)$ plays a role of the design function being symmetric with respect to $x = 0.5$.

Under conditions in Equations (16) and (67), the condition of stationarity $p_0 \to max_y$ takes the following form:

$$y\Big(u_0^2 - 2\lambda\left(1+y^2\right)^2\Big) = 0. \tag{68}$$

The stationarity condition in Equation (68) and the boundary conditions in Equation (16) are satisfied when in the interval $[0, x_*]$ we have:

$$y = 0, \tag{69}$$

which it means that there are no inclusions in that part.

In the interval $[x_*, 0.5]$, the target function satisfies the following algebraic equation:

$$u_0 = \pm\lambda_1\big(1+y^2\big), \tag{70}$$

where $\lambda_1 = \sqrt{2\lambda}$.

Two signs "±" in Equation (70) are responsible for two directions of stability loss (in what follows, the case associated with the sign + is considered).

Using Equation (70), Equation (66) is transformed to the following form:

$$\left(1+y^2\right)_{xx} = -p_0. \tag{71}$$

The symmetry condition for the function $y = y(x)$ regarding the beam center as well as the condition in Equation (69) serve here as boundary condition for the ODE in Equation (71), that is, we have:

$$y\Big|_{x=x_*} = 0; \qquad y_x\Big|_{x=0.5} = 0. \tag{72}$$

The boundary value problem in Equations (71) and (72) while taking into account Equation (69), yields:

$$y^2 = \begin{cases} 0, & x \in [0,\ x_*]; \\ \dfrac{p_0}{2}\left(\left(\dfrac{1}{2}-x_*\right)^2 - \left(\dfrac{1}{2}-x\right)^2\right), x \in \left[x_*, \dfrac{1}{2}\right]. \end{cases} \tag{73}$$

Substituting in Equation (73) into condition in Equation (67) and taking into account symmetry of the function $y = y(x)$, the following formula defining the buckling force is obtained:

$$p_0 = \frac{12\overline{k}}{\left(1-2x_*\right)^3}. \tag{74}$$

Now, substituting Equation (73) into the stationarity condition in Equation (70), one finds the following buckling form in the interval $[x_*, 0.5]$:

$$u_0 = \lambda_1\left(\frac{p_0}{2}\left(\left(\frac{1}{2}-x_*\right)^2 - \left(\frac{1}{2}-x\right)^2\right)+1\right). \tag{75}$$

In the interval $[0,\ x_*]$, the buckling form is defined by the boundary value problem in Equations (66), (69), (16) and (24), which yields:

$$u_0 = \lambda_1\sqrt{1+\frac{p_0}{4}\left(1-2x_*\right)^2}\,sin\sqrt{p_0}x, \quad x \in [0,\ x_*]. \tag{76}$$

Hence, with the help of Equation (74), the equations for x_* takes the following form:

$$\sqrt{1+\frac{3\overline{k}}{1-2x_*}}\,sin\left(2\sqrt{3}\sqrt{\frac{\overline{k}}{\left(1-2x_*\right)^3}}x_*\right) = 1. \tag{77}$$

The numerical results obtained while solving Equation (77) for $\overline{k} = 1-10$ are shown in Figure 7.

From Figure 6, one may conclude that the border zone of the optimal beam does not contain inclusions and it decreases while increasing $\overline{k}$. The dependence of the buckling force p_0 yielded by Equation (74) on $\overline{k}$ for $\overline{k} \in [1, 10]$ is shown in Figure 8.

To estimate efficiency of application of the FG beam of the proposed optimized structure, the buckling force $\overline{p}_0$ of the simply supported composite beam of a regular structure is defined in the following way:

$$\overline{p}_0 = \pi^2(1 + \overline{k}). \tag{78}$$

A comparison of the buckling force p_0 of the FG beam containing the optimized distributed inclusions Equation (74) and the buckling force $\overline{p}_0$ of the beam having the regular structure Equation (78) is presented in Figure 8. Observe that efficiency of application of the optimized distribution of inclusions, beginning from $\overline{k} = 4$, practically does not depend on $\overline{k}$ (Figure 8).

To define the coordinates of the optimized localization of inclusions, $f(x)$ is defined from the following ODE:

$$f'(x) = y^2\overline{k}. \tag{79}$$

The boundary conditions for Equation (79) is:

$$f(0.5) = 0.5. \tag{80}$$

Substituting Equations (73) and (74) into Equation (79) and carrying out the integrations with an account for condition in Equation (80), one obtains:

$$f(x) = \begin{cases} 0, \quad x \in [0,\ x_*]; \\ \dfrac{1}{4}\left(\left(\dfrac{1-2x}{1-2x_*}\right)^3 - 3\dfrac{1-2x}{1-2x_*}\right), x \in \left[x_*, 0.5\right]. \end{cases} \tag{81}$$

Observe that the function $f(x)$ is symmetric with respect to the point (0.5, 0.5) in the interval [0.5, 1].

Equation (81) implies that the optimization process of inclusions distribution is realized via two mechanisms. First, the border zones $[0, x_*]$, $[1 - x_*, 1]$ free from inclusions are

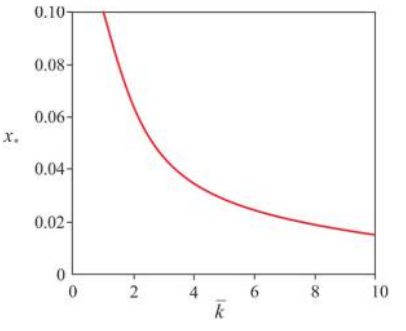

Figure 7.
Dependence of the coordinate x_* on $\overline{k}$

separated. Second, the step between inclusions is changed in a way governed by the target function in Equation (79).

Therefore, the coordinates of optimal inclusions x_i $\left(i = 1 \ldots \frac{n}{2}\right)$ are found from the equation:

$$\frac{1}{4}\left(\left(\frac{1-2x_i}{1-2x_*}\right)^3 - 3\frac{1-2x_i}{1-2x_*}\right) = i\tau, \tag{82}$$

where $\tau = \frac{1}{n}$.

Coordinates of the optimal inclusions x_i $\left(i = \frac{n}{2} + 1 \ldots n\right)$ are symmetric with respect to the point $x = 0.5$. For odd number of inclusions, the inclusion $i = \frac{n}{2}$ does not appear. If $x_* > \tau$, then the coordinates of the first and last inclusions are defined by the following equations:

$$x_1 = x_*, \qquad x_n = 1 - x_*. \tag{83}$$

The remaining inclusion coordinates are defined by Equation (82). Let us find an optimal distribution of the inclusions for $\bar{k} = 10$, $n = 10$. In this case, Equation (77) yields $x_* = 0.015 < \tau = \frac{1}{10}$. It means that the coordinates of all inclusions are defined by Equations (82) and (83).

The function $f(x)$, based on Equation (81), is shown in Figure 9, where also a nomogram useful for a graphic determination of the optimized inclusions coordinate x_i (i = 1,. . .,5) (symmetric with respect to x = 0.5) is presented. Numerical values of the optimized coordinates $x_i(i$ = 1,. . .,5) are yielded by Equation (82) for the following parameters: i = 1,. . .,5; $x_* = 0.015$; $\tau = \frac{1}{10}$.

The optimized structure of the FG beam found with the help of Equation (82) is shown in Figure 10b, whereas Figure 10a reports the structure of an equivalent regular composite beam.

The buckling force of the simply supported beam of an optimized structure (Figure 10b) is 21.59 per cent higher than the corresponding buckling force for the regular beam (Figure 10a). Figure 11 shows the buckling forms of the composite beam with the optimized structure defined by Equation (82) and (83) and with a regular structure.

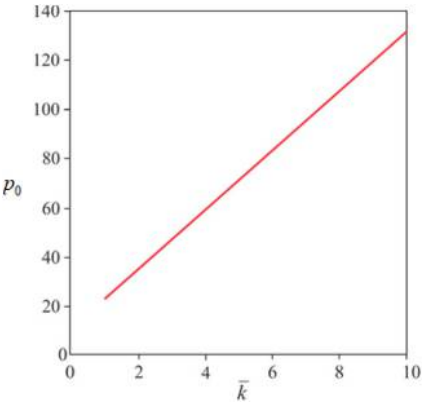

Figure 8.
Dependence of the buckling force p_0 on $\bar{k}$

Finally, let us analyze possibility of local buckling for the beam shown in Figure 10b. Low bound of the local buckling force $\tilde{p}$ on the interval $[0, x_1]$ can be determined using a beam of the length $x_1 = 0.195$, where x_1 is given by Equation (82): $\tilde{p} = \frac{\pi^2}{x_1^2} = 259.55$. The general buckling force defined by Equation (82) yields $p_0 = 131.88$, so, $p_0 < \tilde{p}$.

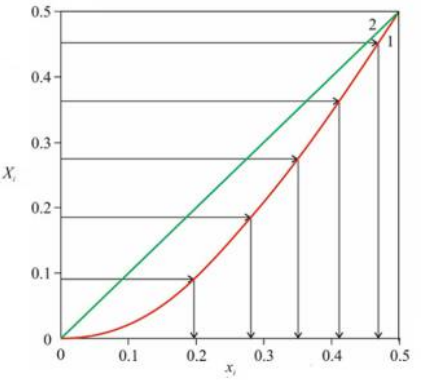

Figure 9.
Nomogram for the graphical determination of the optimized coordinates of inclusion x_i (i = 1,. . .,5) for $\bar{k} = 10$, $n = 10$, $\tau = 0.091$, $x_i = i\tau$ if the coordinates of inclusions are regularly distributed

Note: Curve 1 denotes the function y = $f(x)$, whereas the straight Line 2 denotes y = x)

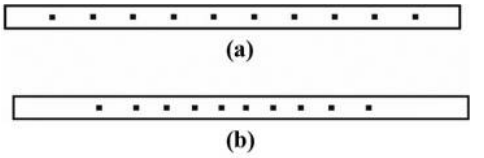

Figure 10.
Two-component beam

Notes: (a) regular structure; (b) optimized structure (n ¼ 10; k ¼ 10)

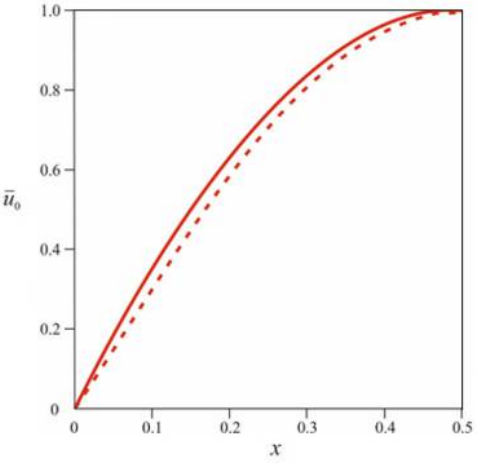

Figure 11.
Buckling form $\bar{u}_0$ ($\bar{u}_0 = u_0(x)/u_0(1/2)$) of the FG beam with optimized structure (solid curve) versus the buckling form of the regular two-components beam (dashed curve) for $\bar{k} = 1$, $n = 10$

4. Concluding remarks

Separation of the FG beams into structures with regularly distributed inclusions of variable cross-section and with irregularly distributed inclusions of constant cross-section has shown its effectiveness. It allowed for formulating and solving the problem of optimization of the internal structure of the FG beam while studying its stability problem. Employment of the homogenization method allowed one to reduce a class of the required functions to a class of piece-wise continuous functions. The adequacy of FG homogeneous models increases with increasing number of inclusions. The latter enabled us to apply the well-known variational methods.

The optimized internal structures of the FG beam with inclusions of the variable size and with the non-constant step are similar to each other. They are characterized by occurrence of the border zones being free of inclusions and exhibiting the inclusions of the biggest size in the central zone of the beam. However, this implies a potential local buckling in the border zones, which requires a separate analysis for each of the developed optimal designs.

Remarkably, the final result of the carried out optimization of the internal structure for both studied types of FGM are similar. The relative increase in the buckling force of the FG beam with the optimized internal structure is on amount of 20 per cent while comparing it with the regular structure beam.

The use of Rayleigh relations in Equations (19)-(21) as stationarity conditions allows us to obtain optimal solutions for the problem under consideration with an account of arbitrary boundary conditions. On the other hand, the analysis of the influence of boundary conditions optimal FG rods behavior stands for one of the promising directions for further research.

Another important area of further research is that devoted to study a combination of the two schemes of the considered optimal design. The main difficulty here is the impossibility to use two different objective functions. One of the possible schemes to avoid the occurred problem is the use of sequential optimization. First, the optimum distribution of the volumes of the inclusions can be determined, and then their optimal localization should be carried out.

In addition, it is of interest to study the dual problem (Sanchez-Palencia, 1980) where minimization of the volume of inclusions at a constant (given) value of the buckling force is provided.

In conclusion, it should be noticed that even in cases where for reasons of high cost or difficulties of technological nature the possibilities of creating FG designs of optimal structure are limited, the study of optimal design structures is of practical importance, as it allows us to theoretically assess the quality of traditional non-optimal structures.

References

Alfutov, N.A. (2000), *Stability of Elastic Structures*, Springer, Berlin.

Andrianov, I.V., Awrejcewicz, J. and Diskovsky, A.A. (2005), "Homogenization of the irregular cell-types constructions", in Awrejcewicz, J., Sendkowski, D., Mrozowski, J. (Eds), Proceedings 8th Conference on Dynamical Systems – Theory and Applications, *Lodz*, pp. 871-876.

Andrianov, I.V., Awrejcewicz, J. and Diskovsky, A.A. (2006), "Homogenization of quasiperiodic structures", *Transaction ASME Journal of Vibration and Acoustics*, Vol. 128 No. 4, pp. 532-534.

Andrianov, I.V., Awrejcewicz, J. and Diskovsky, A.A. (2009), "Asymptotic investigation of corrugated elements with quasi-periodic structures", in Awrejcewicz, J., Kaźmierczak, M., Olejnik, P., Mrozowski, J., (Eds), Proceedings 10th Conference on Dynamical Systems – Theory and Applications, *Lodz*, pp. 523-532.

Andrianov, I.V., Awrejcewicz, J. and Diskovsky, A.A. (2011), "Homogenization of the functionally-graded materials", in Awrejcewicz, J., Kaźmierczak, M., Olejnik, P. and Mrozowski, J. (Eds), *Proceedings 11th Conference on Dynamical Systems – Theory and Applications*, Lodz, pp. 55-62.

Andrianov, I.V., Awrejcewicz, J. and Diskovsky, A.A. (2013), "Sensitivity analysis in design of constructions made of functionally-graded materials", *Proceedings of the Institution of Mechanical Engineers, Part C: Journal of Mechanical Engineering Science*, Vol. 227 No. 1, pp. 19-28.

Andrianov, I.V., Awrejcewicz, J. and Diskovsky, A.A. (2017), "Functionally graded rod with small concentration of inclusions: homogenization and optimization", *International Journal of Non-Linear Mechanics*, Vol. 91, pp. 189-197.

Andrianov, I.V., Awrejcewicz, J. and Diskovsky, A.A. (2010), "Design of the non-homogeneous quasi-regular structures", in Bolshakov, V.I. and Weichert, D. (Eds), *Advanced Problems in Mechanics of Heterogeneous Media and Thin-walled Structures*, ENEM, Dnipropetrovsk, pp. 7-18.

Andrianov, I.V., Awrejcewicz, J. and Manevitch, L.I. (2004), *Asymptotical Mechanics of Thin-Walled Structures: A Handbook*, Springer, Berlin, Heidelberg.

Andrianov, I.V. and Piskunov, V.I. (1997), "Stability of ribbed plates with allowance for the discrete arrangement", *Mechanics of Solids*, Vol. 32 No. 6, pp. 135-141.

Anthoine, A. (2010), "Second-order homogenisation of functionally graded materials", *International Journal of Solids and Structures*, Vol. 47 Nos 11/12, pp. 1477-1489.

Babushka, I. (1979), "The computation aspects of the homogenization problem", *Lecture Notes Mathematics*, Vol. 704, pp. 309-316.

Bakhvalov, N.S. and Panasenko, G.P. (1989), "Averaging processes in periodic media", *Mathematical Problems in Mechanics of Composite Materials*, Kluwer, Dordrecht.

Banichuk, N.V. (1990), *Introduction to Optimization of Structures*, Springer, New York, NY.

Bensoussan, A., Lions, J.-L. and Papanicolaou, G. (1978), *Asymptotic Analysis for Periodic Structures*, North-Holland, Amsterdam.

Cadman, J., Zhou, S., Chen, Y. and Li, Q. (2012), "On design of multi-functional microstructural materials", *Journal of Materials Science*, Vol. 48 No. 1, pp. 51-66.

Elishakoff, I. (2005), *Eigenvalues of Inhomogeneous Structures: Unusual Closed-Form Solutions*, CRC Press, Boca Raton.

Fish, J. and Chen, W. (2001), "A dispersive model for wave propagation in periodic heterogeneous media based on homogenization with multiple spatial and temporal scales", *Journal of Applied Mechanics*, Vol. 68, pp. 153-161.

Fish, J. and Chen, W. (2004), "Space–time multiscale model for wave propagation in heterogeneous media", *Computer Methods in Applied Mechanics and Engineering*, Vol. 193 Nos 45/47, pp. 4837-4856.

Huang, Y. and Li, X.F. (2010), "Buckling analysis of nonuniform and axially graded columns with varying flexural rigidity", *Journal of Engineering Mechanics*, Vol. 137 No. 1, pp. 73-81.

Keller, J.B. (1960), "The shape of the strongest column", *Archive for Rational Mechanics and Analysis*, Vol. 5 Nos 1/4, pp. 275-285.

Keller, J.B. and Niordson, F.I. (1966), "The tallest column", *Indiana University Mathematics Journal*, Vol. 16 No. 5, pp. 433-446.

Kolpakov, A.G. (2004), *Stressed Composite Structures: Homogenized Models for Thin-Walled Nonhomogeneous Structures with Initial Stresses*, Springer, Berlin, New York, NY.

Li, H., Luo, Z., Gao, L. and Qin, Q. (2018a), "Topology optimization for concurrent design of structures with multi-patch microstructures by level sets", *Computer Methods in Applied Mechanics and Engineering*, Vol. 331, pp. 536-561.

Li, H., Luo, Z., Gao, L. and Walker, P. (2018b), "Topology optimization for functionally graded cellular composites with metamaterials by level sets", *Computer Methods in Applied Mechanics and Engineering*, Vol. 328, pp. 340-364.

Manevitch, L.I., Andrianov, I.V. and Oshmyan, V.G. (2002), *Mechanics of Periodically Heterogeneous Structures*, Springer, Berlin, Heidelberg, New York, NY.

Mikhlin, S.G. (1964), *Variational Methods in Mathematical Physics*, Pergamon Press, Oxford.

Movchan, A.B., Movchan, N.V. and Poulton, C.G. (2002), *Asymptotic Models of Fields in Dilute and Densely Packed Composites*, Imperial College Press, London.

Olhoff, N. and Rasmussen, S.H. (1977), "On single and bimodal optimum buckling loads of clamped columns", *International Journal of Solids and Structures*, Vol. 13 No. 7, pp. 605-614.

Panasenko, G.P. (2005), *Multi-Scale Modeling for Structures and Composites*, Springer, Berlin.

Radman, A., Huang, X. and Xie, Y.M. (2013), "Topology optimization of functionally graded cellular materials", *Journal of Materials Science*, Vol. 48 No. 4, pp. 1503-1510.

Ramu, I. and Mohanty, S.C. (2014), "Vibration and parametric instability of functionally graded material plates", *Journal of Mechanical Design and Vibration*, Vol. 2 No. 4, pp. 102-110.

Reiter, T., Dvorak, G. and Tvergaard, V. (1997), "Micromechanical models for graded composite materials", *Journal of Mechanical Physics and Solids*, Vol. 45 No. 8, pp. 1281-1302.

Sanchez-Palencia, E. (1980), *Non-Homogeneous Media and Vibration Theory*, Springer, Berlin.

Shahba, A. and Rajasekaran, S. (2012), "Free vibration and stability of tapered euler–Bernoulli beams made of axially functionally graded materials", *Applied Mathematical Modelling*, Vol. 36 No. 7, pp. 3094-3111.

Singh, K.V. and Li, G. (2009), "Buckling of functionally graded and elastically restrained non-uniform columns", *Composites: Part B*, Vol. 40 No. 5, pp. 393-403.

Sun, X., Zhou, Ch., Ichchou, M., Lainé, J.-P. and Zine, A.-M. (2017), "Multi-scale homogenization of transversal waves in periodic composite beams", *International Journal of Applied Mechanics*, Vol. 9 No. 3, p. 1750039.

Suresh, S. and Mortensen, A. (1998), *Fundamentals of Functionally Graded Materials*, Cambridge University Press, Cambridge.

Tadjbakhsh, I. and Keller, J.B. (1962), "Strongest columns and isoperimetric inequalities for eigenvalues", *Journal of Applied Mechanics*, Vol. 29 No. 1, pp. 159-164.

Victor, B. and Larry, W.B. (2007), "Modelling and analysis of functionally graded materials and structures", *Applied Mechanics Review*, Vol. 60, pp. 195-203.

Wang, Q., Varadan, V.K. and Quek, S.T. (2006), "Small scale effect on elastic buckling of carbon nanotubes with nonlocal continuum models", *Phys Lett A*, Vol. 357 No. 2, pp. 130-135.

Wang, C.M., Wang, C.Y. and Reddy, J.N. (2005), *Exact Solutions for Buckling of Structural Members*, CRC Press, Boca Raton.

Xing, Y.F. and Chen, L. (2014a), "Accuracy of multiscale asymptotic expansion method", *Composite Structures*, Vol. 112, pp. 38-43.

Xing, Y.F. and Chen, L. (2014b), "Physical interpretation of multiscalt asymptotic expansion method", *Composite Structures*, Vol. 116, pp. 694-702.

Yilmaz, Y., Girgin, Z. and Evran, S. (2013), "Buckling analyses of axially functionally graded nonuniform columns with elastic restraint using a localized differential quadrature method", *Mathematical Problems of Engineering*, Vol. 2013, pp. 1-12.

Zhang, Y.Q., Liu, G.R. and Han, X. (2006), "Effect of small length scale on elastic buckling of multi-walled carbon nanotubes under radial pressure", *Physics Letters A*, Vol. 349 No. 5, pp. 370-376.

Zhou, S. and Li, Q. (2008), "Design of graded two-phase microstructures for tailored elasticity gradients", *Journal of Materials Science*, Vol. 43 No. 15, pp. 5157-5167.

Appendix

Let us estimate an error of the employed homogenization approach. This problem has been already considered in the case of statics (Xing and Chen, 2014) and dynamics (Wang *et al.*, 2006; Sun *et al.*, 2017), where the problems were solved by the homogenization approach and FEM. The comparison of the obtained results confirm a physically obvious conclusion: the global characteristics (the energy of the system associated with the lower part of the vibration spectrum) are determined by homogenization approach with a high accuracy. However, in our paper, we consider the problem of stability. We show, following the paper (Andrianov and Piskunov, 1997), that the first eigenvalue of the corresponding eigenvalue problem defined by homogenization approach is obtained with accuracy of ε^2.

Consider the eigenvalue problem:

$$a\left(\frac{x}{\varepsilon}\right)\frac{d^2u}{dx^2}+pu=0, \tag{A1}$$

$$u=0 \quad \text{at} \quad x=0, x=1. \tag{A2}$$

Using fast and slow variables and taking into account the relation:

$$\frac{d}{dx}=\frac{\partial}{\partial x}+\varepsilon^{-1}\frac{\partial}{\partial \eta} \tag{A3}$$

we obtain a PDE instead of the original ODE. We seek its solution as the series with regard to the parameter ε of both u and p:

$$u=u_0(\eta,x)+\varepsilon u_1(\eta,x)+\varepsilon^2 u_2(\eta,x)+\ldots, \tag{A4}$$

$$p=p_0+\varepsilon p_1+\varepsilon^2 p_2+\ldots. \tag{A5}$$

Substituting the expansions in Equations (A4) and (A5) into the original eigenvalue problem in Equations (A1) and (A2), one gets:

$$u_0\equiv u_0(x), \qquad u_1\equiv u_1(x), \tag{A5}$$

$$a\frac{\partial^2 u_2}{\partial \eta^2}+a\frac{d^2u_0}{dx^2}+p_0u_0=0, \tag{A6}$$

$$\frac{\partial^2 u_3}{\partial \eta^2}+2\frac{\partial^2 u_2}{\partial x\partial \eta}+\frac{d^2u_1}{dx^2}+a^{-1}p_1u_0+a^{-1}p_0u_1=0, \tag{A7}$$

...

$$u_i=0, \qquad i=0,1,2,\ldots \qquad \text{at}\, x=0, \qquad x=1. \tag{A8}$$

Homogenization of Equation (A5) leads to the following result:

$$\tilde{a}\,\frac{d^2u_0}{dx^2}+p_0u_0=0;\qquad \tilde{a}\;=\left[\int_0^1 a^{-1}d\,\eta\right]^{-1}.. \tag{A9}$$

Solution of the eigenvalue problem in Equations (A9) and (A8) is as follows:

$$p_0=\pi^2\tilde{a};\; u_0=C\sin\pi x. \tag{A10}$$

For the first fast corrector term, one gets:

$$u_2=\left[\tilde{a}\int_0^{\eta}\left(\int_0^{\eta}a^{-1}d\,\eta\right)d\,\eta-0.5\,\eta^2-C_1\,\eta\right]\frac{d^2u_0}{dx^2};\qquad C_1=\tilde{a}\int_0^1\left(\int_0^{\eta}a^{-1}d\,\eta\right)d\,\eta-0.5. \tag{A11}$$

It is important to note that the first fast corrector satisfies the boundary conditions in Equation (A8), and hence, that a boundary layer is absent.

Substituting Equation (A11) to Equation (A7) yields:

$$\frac{\partial^2u_3}{\partial\,\eta^2}+\frac{d^2u_1}{dx^2}+a^{-1}p_1u_0+a^{-1}p_0u_1=2\left(\eta+C_1-\tilde{a}\int_0^{\eta}a^{-1}d\,\eta\right)\frac{d^3u_0}{dx^3}. \tag{A12}$$

Homogenization of Equation (A12) gives:

$$\frac{d^2u_1}{dx^2}+\tilde{a}^{-1}p_1u_0+\tilde{a}^{-1}p_0u_1=0. \tag{A13}$$

Multiplication of Equation (A13) by u_0, carrying out the integration and taking into account self-adjointness of the eigenvalue problem in Equations (A9) and (A8), one obtains:

$$p_1=0. \tag{A14}$$

Therefore, we have shown that indeed the homogenization approach gives possibility to compute the eigenvalue with accuracy of ε^2.

Corresponding author
Jan Awrejcewicz can be contacted at: jan.awrejcewicz@p.lodz.pl